J Appl Electrochem (2017) 47:237–248
DOI 10.1007/s10800-016-1029-y

RESEARCH ARTICLE

Multifunctional macromolecular design as a self-standing electrolyte for high-temperature single-ion lithium batteries

Yongqin Wang[1,2] · Yanwu Zhang[1] · Hongjun Hou[2]

Received: 23 September 2016 / Accepted: 8 December 2016 / Published online: 19 December 2016

Abstract A macromolecular electrolyte is designed with different chemical moieties to perform different functions, and it is extremely suitable to be applied in solid high-temperature lithium ion batteries. The preparation of the electrolyte involves synthesis of a comb-like macromolecule and immobilization of lithium ions. The comb-like macromolecule is synthesized via a ring-opening metathesis copolymerization of norbornene derivatives anchored with phosphate and polyethylene glycol monomethyl ether ($–O(CH_2CH_2O)_nCH_3$) and is partially cross-linked through polyethylene glycol ($–(CH_2CH_2O)_n–$) bridge. The immobilization of lithium ions is carried out by lithium bis(trifluoromethyl-sulfonyl)imide. The as-prepared electrolyte membrane has a bicontinuous morphology consisting of a cross-linked mechanical scaffold intertwined with continuous Li^+ ions conducting channels. Apart from lithium ion transference number close to unity and remarkable ionic conductivity, the electrolyte also displays strong strength, high flexibility, good thermal stability and outstanding flame retardancy. At 80 °C, $LiFePO_4$/macromolecular electrolyte/Li coin cells, with the discharge capacity of 134.1 mAh g^{-1} at a current density of 0.2 C, are able to maintain a value of 120.7 mAh g^{-1} after 100 cycles of charge and discharge.

Graphical Abstract Monodisperse and multifunctional copolymer is prepared via ring-opening metathesis copolymerization and modified to be used as a single-ion electrolyte for lithium ion batteries. The as-synthesized electrolyte involves a bicontinuous morphology consisting of a cross-linked mechanical scaffold intertwined with continuous Li^+ ions conducting channels, resulting in outstanding high-temperature electrochemical performance.

Electronic supplementary material The online version of this article (doi:10.1007/s10800-016-1029-y) contains supplementary material, which is available to authorized users.

✉ Yanwu Zhang
zhangyanwu@zzu.edu.cn

[1] School of Chemical Engineering and Energy, Zhengzhou University, Zhengzhou 450001, People's Republic of China

[2] Do-Fluoride Chemicals Co. Ltd., Jiaozuo 454191, People's Republic of China

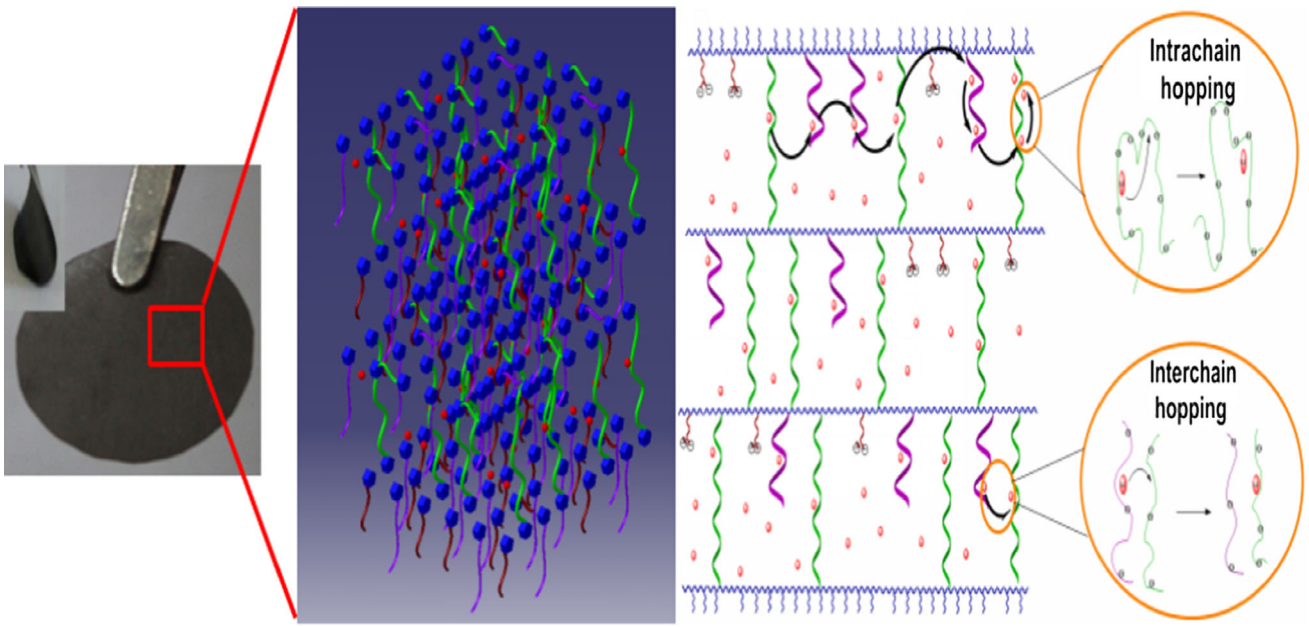

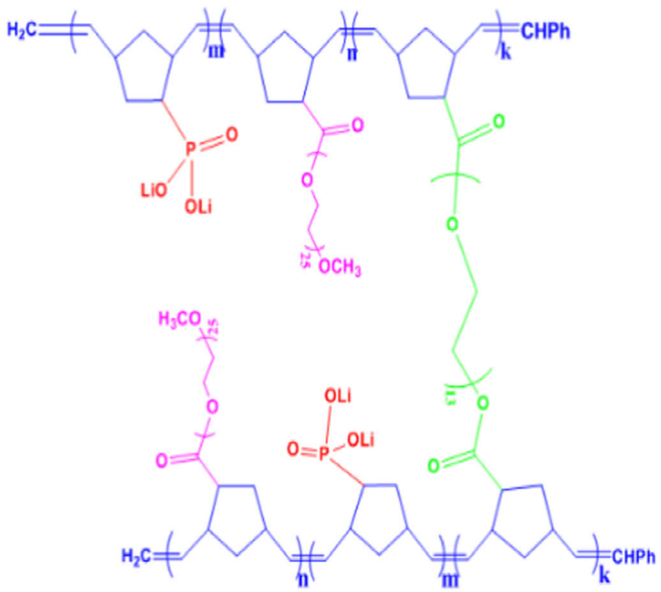

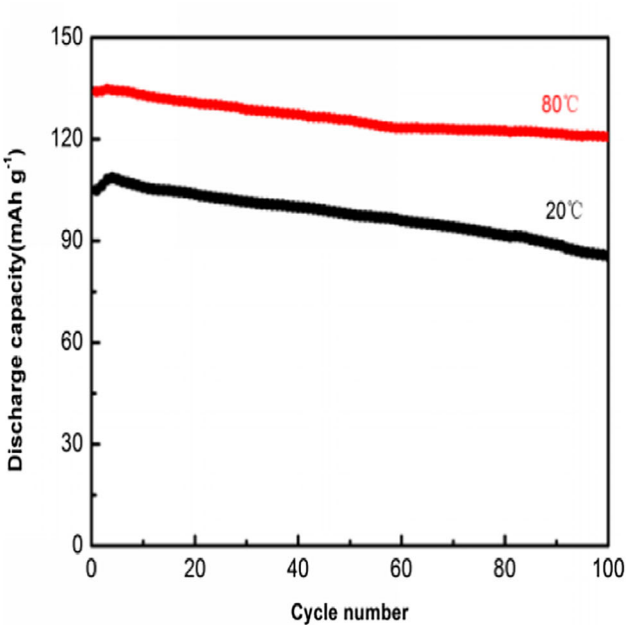

Keywords Multifunctional macromolecular electrolyte · Ring-opening metathesis copolymerization · High temperature · Single-ion lithium batteries

1 Introduction

For commercially available lithium ion batteries (LIBs), organic solvents are generally incorporated into electrolytes, which results in leakage, flammability and even explosion. Therefore, solid-state polymer electrolytes (SPEs) appear to be a promising candidate to alleviate safety issues related to liquid electrolytes, due to their intrinsic properties of design flexibility, no liquid leakage and mechanical properties [1, 2]. Li^+ ions in these SPEs are primarily conducted with the swing of polymer chains through inter- and intra-chain hopping mechanism in amorphous regions [3, 4].

By now, PEO-based SPEs are most studied because of strong Li^+ solvating ability and chain flexibility [5, 6]. However, semicrystalline morphology of PEO hinders its practical application in SPEs [7]. To enhance the ionic conductivity, various approaches including addition of plasticizers [8–11], blending of polymers [12–16] and designing of copolymers (CP) [17–19] have been put

forward to suppress the crystallinity of PEO-based electrolytes. In the long-term operation, successive charge–discharge cycles, temperature changes, pressure varieties and chemical reactions usually trigger macrophase separation of solid-state polymer electrolytes resulting in poor cycling performance of LIBs [20–22]. In order to avoid the multicomponent mixtures and complicated phase behavior, CP is considered to be the most effective way to offer both high ionic conductivity and dimensional stability [23–25].

In dual-ion conductor electrolytes, Li^+ ions are incorporated into electrolytes by doping inorganic lithium salts into copolymers. But the concentration polarization is the typical feature observed in such systems [4, 26, 27]. Thus, an improved system defined as single-ion polymer electrolyte (SIPE) has become an intriguing domain of recent researches, in which anions are chemically attached onto polymer chains [28–31]. Furthermore, the perfect design of SIPE should contain three different functional domains: the source providing Li^+ ions, the pathway facilitating Li^+ ions conduction and self-supporting area.

Among various polymerization methods, a ring-opening metathesis polymerization can generate diverse macromolecules tailored by the functional groups substituted at the backbone. Therefore, multifunctional copolymers can be prepared to afford solid electrolytes through a ring-opening metathesis copolymerization (ROMCP) of norbornene derivatives. Herein, a copolymer anchored with phosphate and polyethylene glycol monomethyl ether ($–O(CH_2CH_2O)_nCH_3$) was first prepared and cross-linked through polyethylene glycol ($–(CH_2CH_2O)_n–$) bridges via ring-opening metathesis copolymerization. Subsequently, the copolymer was immobilized with Li^+ ions to achieve a single-ion macromolecular electrolyte (SIME). In SIME, phosphate lithium with flame-retardant superiority can provide Li^+ ions and the segment $–O(CH_2CH_2O)_nCH_3$ of high chain flexibility can promote Li^+ ions transportation. Through cross-linking of $–(CH_2CH_2O)_n–$ bridges, SIME can obtain mechanical support and suppress the crystallization of PEO. The morphology, electrochemical properties and other properties of SIME including thermal stability, mechanical property and flame-retarding property were studied in this paper. What is more, coin cell with $LiFePO_4$ as the cathode and Li metal as the counter electrode was assembled with SIME and its performance especially at 80 °C was demonstrated.

2 Experimental

2.1 Materials

The second-generation Grubbs catalyst (Sigma-Aldrich), ethyl vinyl ether (98%, TCI), bromotrimethylsilane (98%, J&K), lithium bis(trifluoromethyl-sulfonyl)imide (LiTFSI, 99.0%, Sigma-Aldrich) and bromotrimethylsilane (98%, Acros) were used as received. Dichloromethane (DCM) was dried over CaH_2 and used after reduced pressure distillation under nitrogen. All the other reagents were of chromatography grade and directly used without purification. 5-Norbornene-2-dimethyl phosphonate (M1), 5-norbornene-2-poly(ethylene glycol) monoester(M2), cross-linker bi-norbornene grafted poly(ethylene glycol) (M3) were synthesized as described in Scheme S1.

2.2 Synthesis of copolymer (PM1-co-PM2-co-PM3)

The second-generation Grubbs' catalyst (5.66 mg) was dissolved in dry DCM (1.33 mL) and stirred for 15 min, followed by a solution of M1 (202.19 mg), M2 (217.54 mg) and M3 (46.5 mg) in dry DCM (30 mL). The reaction was allowed to stir at 25 °C until the solution color changed from pink to dark brown. At time intervals, 0.5 mL of the solution was taken out per hour and quenched with 600 equiv of ethyl vinyl ether for monitoring the monomer conversion by GPC. The polymerization was terminated by the addition of 600 equiv of ethyl vinyl ether. After evaporated under reduced pressure, a green solid (85% yield) was obtained.

2.3 Synthesis of PM1S-co-PM2-co-PM3

PM1-co-PM2-co-PM3 and bromotrimethylsilane were, respectively, dissolved in DCM (5 mL). Then, these two solutions were mixed and stirred for additional 16 h at room temperature. Finally, methanol was added and the stirring continued for 24 h (the molar ratio between phosphate, bromotrimethylsilane and methanol was 1:2:4). PM1S-co-PM2-co-PM3 was isolated by evaporating the solvent.

2.4 Preparation of SIME

LiTFSI (0.287 g) and PM1S-co-PM2-co-PM3 (2.349 g) were dissolved in DMF (20 mL) and stirred at 90 °C for 24 h under N_2. Then, the resulted bis (trifluoromethylsulfonyl) imide was removed by vacuum. Subsequently, the mixture was drop-cast into a Teflon Petri dish and dried in an oven at 30 °C for 24 h to evaporate the DMF solvent. The obtained membrane was further dried under vacuum at 60 °C for 24 h to remove a trace amount of DMF. The membrane was punched to obtain a circular shape for use. The thickness of SIME was determined by its quantity and diameter of the Teflon plate.

2.5 Methods

Gel permeation chromatography (GPC) analysis was carried out with Agilent 1100 series equipped with a RI-

G1362A detector and a PL gel Mixed-C column using DMF as the mobile phase at a flow rate of 1.0 mL min^{-1}. Polymer molecular weights and molecular weight distributions were estimated on the basis of the calibration curve obtained by polystyrene standards. ^{1}H-NMR spectra (400 MHz) were recorded on a Bruker AV 400 spectrometer, using CD_3COCD_3 as the solvent at 25 °C. Thermal gravimetric analysis (TGA) was performed on a Mettler Toledo TGA system at 5 °C min^{-1} from room temperature to 500 °C under a flow of nitrogen. The surface morphology of the prepared SIME was investigated by JSM-7500F scanning electron microscopy (SEM). The stress–strain test was measured on a Shimadzu AG-50 kN universal tester. The crosshead speed was set at 1 mm min^{-1}. The width of the sample was 8 mm, and the length was 60 mm. The thickness of SIME was measured with a micrometer (SM & CTW, Shanghai).

Ionic conductivity was measured by electrochemical impedance spectroscopy (EIS) using a Zahner Zennium electrochemical station. SIME was sandwiched between two stainless steel plate electrodes. Impedance data were measured in the frequency range of 10^6 to 0.1 Hz with an oscillating voltage of 10 mV at selected temperatures. Before the EIS analysis, the SIME-fitted device was heated at 60 °C for 2 h. Ionic conductivity of SIME was calculated using the following equation: $\sigma = l/(RS)$, where σ is the ionic conductivity, l denotes the thickness of SIME, R stands for the bulk resistance and S represents the surface area.

Linear sweep voltammetry (LSV) was carried out with a stainless steel used as the working electrodes and a lithium foil used as the counter and reference electrode. The measurement was carried out between 2.0 and 6.0 V (vs. Li^+/Li) with a scan rate of 1 mV s^{-1}. Prior to test, the cell was stabilized for 2 h at each temperature.

Lithium ion transference number (T_{Li^+}) was measured by sandwiching SIME between two lithium electrodes. A DC potential of 10 mV was applied until a steady state was reached.

To analyze the battery performance, coin cells assembled with SIME as the separator and electrolyte were measured at 20 and 80 °C. The $LiFePO_4$ working electrode was prepared by coating a N-methyl-2-pyrrolidone (NMP)-based slurry containing $LiFePO_4$, acetylene black and PVDF in a weight ratio of 8:1:1 on aluminum foil using the doctor blade technique, and the cast foils were subsequently dried in a vacuum oven at 80 °C for 12 h. The dried cathode was then cut into a circular shape for use. The Li metal was used as anode, and the assembling of the standard coin cells (CR2025) was carried out inside a glove box. Battery cycling experiment was performed at 0.2 C-rate on a Land CT2001A battery tester between 2.7 and 4.2 V based on the $LiFePO_4$ cathode. When conducted at 80 °C, the sample was preheated for 2 h to guarantee the consistent temperature from the inside out.

3 Results and discussion

The synthetic importance of the design is strongly encouraged by the interaction between ether oxygen atoms and Li^+ ions, as well as low dissociation and retardant property of phosphate group. Because the copolymer (PM1-co-PM2) cannot form a self-standing membrane, the cross-linker (M3) is introduced into the PM1-co-PM2 with various ratios to form SIME. Confirmed by numerous experiments, the as-synthesized SIME has both excellent mechanical strength and reasonable flexibility when the ratio of M1, M2 and M3 is set as 4:1:1.

3.1 Molecular structure of PM1-co-PM2-co-PM3, PM1S-co-PM2-co-PM3 and PM1Li-co-PM2-co-PM3

The molecular weights of PM1, PM2, PM3, PM1-co-PM2 and PM1-co-PM2-co-PM3 are characterized by GPC, and their GPC traces are shown in Fig. 1. The shift of characteristic peaks to left after the copolymerization indicates that copolymer of higher molecular weight is prepared. In ^{1}H-NMR spectra (Fig. 2), the disappearance of chemical shifts at 6.2–5.9 ppm ascribing to double bands in

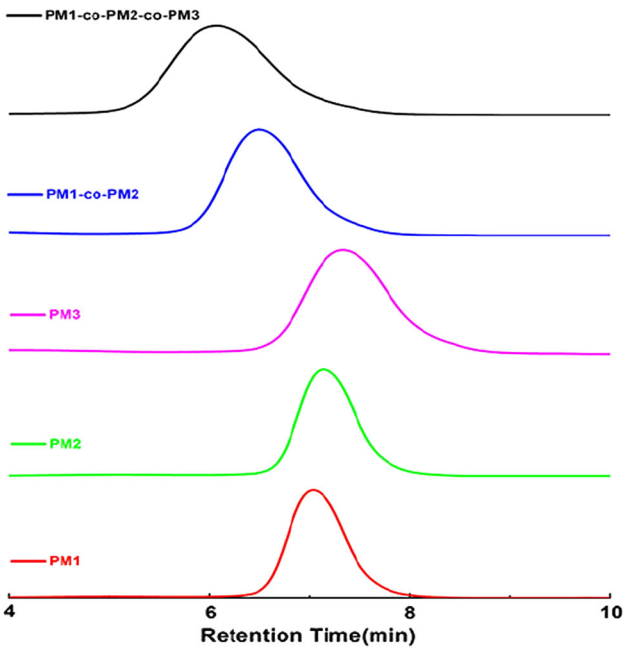

Fig. 1 GPC analysis of PM1-co-PM2-co-PM3 (Mn = 9×10^4, PDI = 1.88), PM1-co-PM2 (Mn = 6.39×10^4, PDI = 1.51), PM3 (Mn = 2.78×10^4, PDI = 1.58), PM2 (Mn = 3.08×10^4, PDI = 1.32), PM1 (Mn = 2.98×10^4, PDI = 1.28)

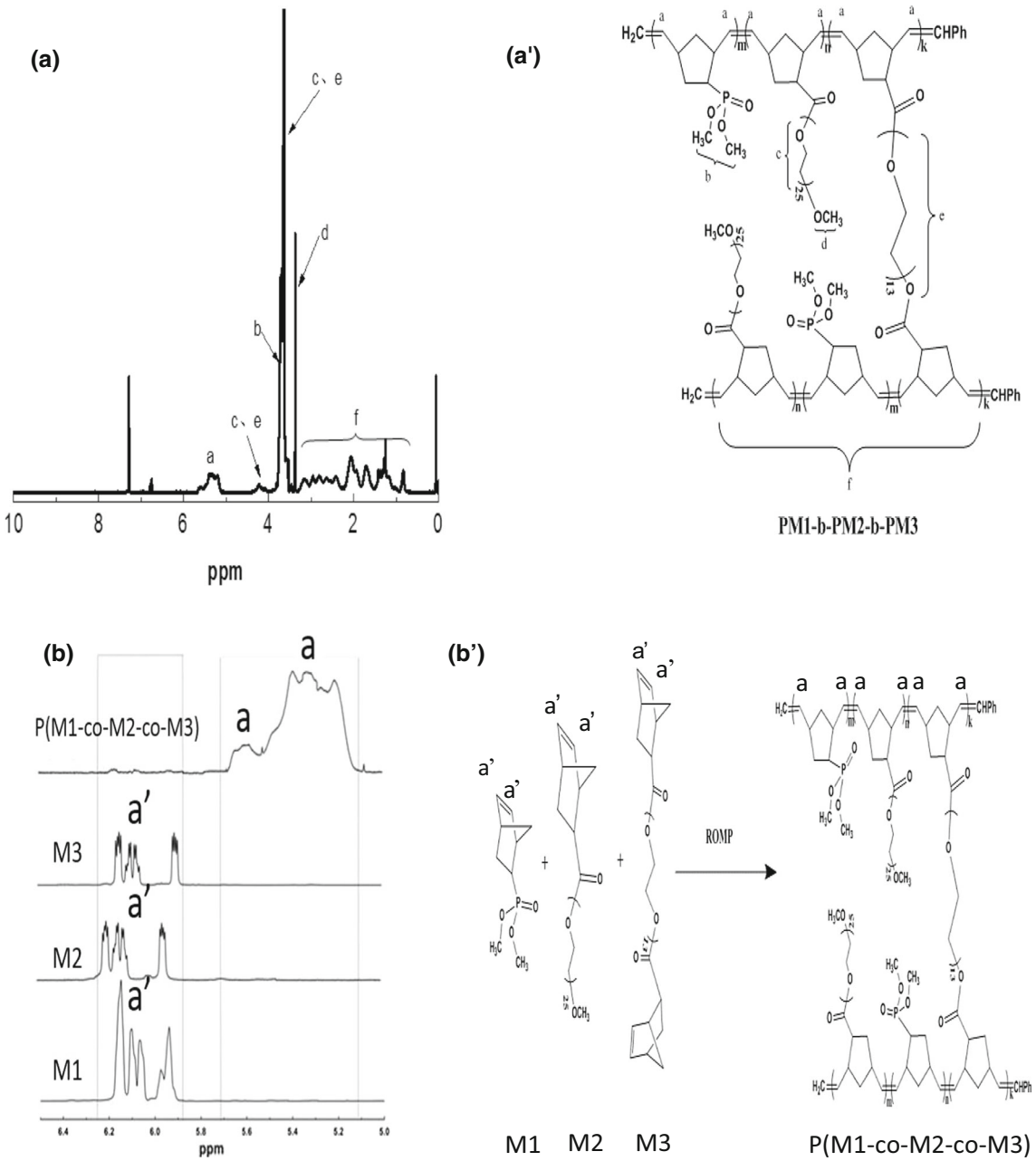

Fig. 2 **a** Full ^{1}H NMR spectrum and **a**′ structure of PM1-co-PM2-co-PM3, **b** magnified spectra in directions *x* and *y* (disappearance of the norbornene cyclic protons and appearance of the internal double bond protons) and **b**′ the corresponding ROMP reaction

monomers and the formation of new shifts at 5.2–5.8 ppm after ROMCP further confirm that monomers of M1, M2, M3 are incorporated into chains of PM1-co-PM2-co-PM3.

Synthesis of PM1S-co-PM2-co-PM3 and immobilization of Li^{+} ions are illustrated in Scheme 1. In ^{1}H-NMR spectra (Fig. 3), the disappearance of chemical shift at 3.55–3.65 ppm ascribing to –*P*–OC***H***$_3$ and the formation of new shifts at 4.17–4.2 ppm ascribing to –P–O***H*** indicate that PM1S-b-PM2-b-PM3 is successfully synthesized after hydrolysis using trimethylsilyl bromide. The immobilization of Li^{+} ions is also proved by the disappearance of shifts at 4.17–4.2 ppm ascribing to –P–O***H***.

3.2 Morphology and physical properties of SIME

As shown in Fig. 4a, b, SIME displays high flexibility and uniform surface. Simultaneously, SIME involves a bicontinuous morphology consisting of a cross-linked domain intertwined with continuous Li^{+} ions conducting channels (Fig. 4c) which imparts an exceptional combination of

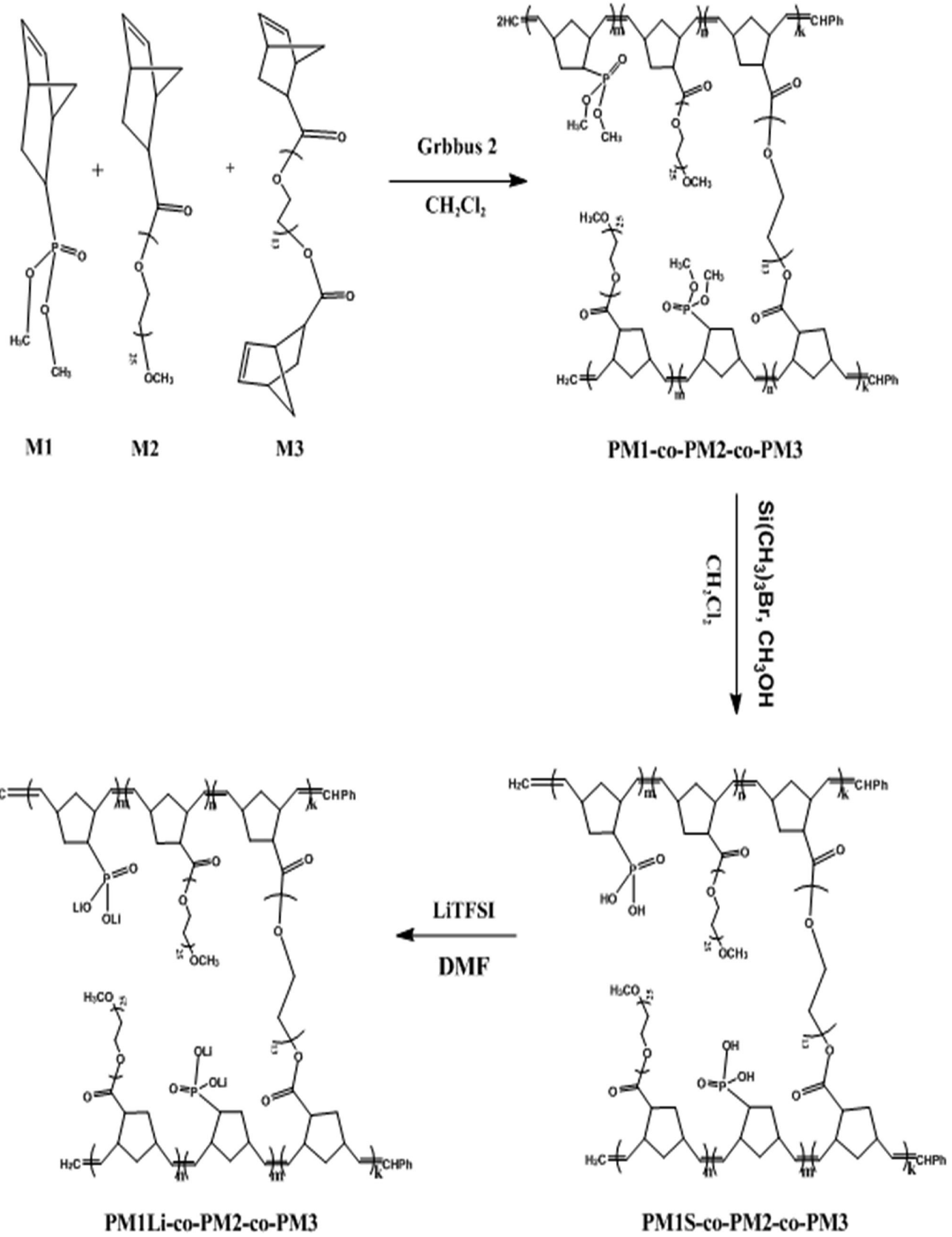

Scheme 1 Procedure for the synthesis of SIME

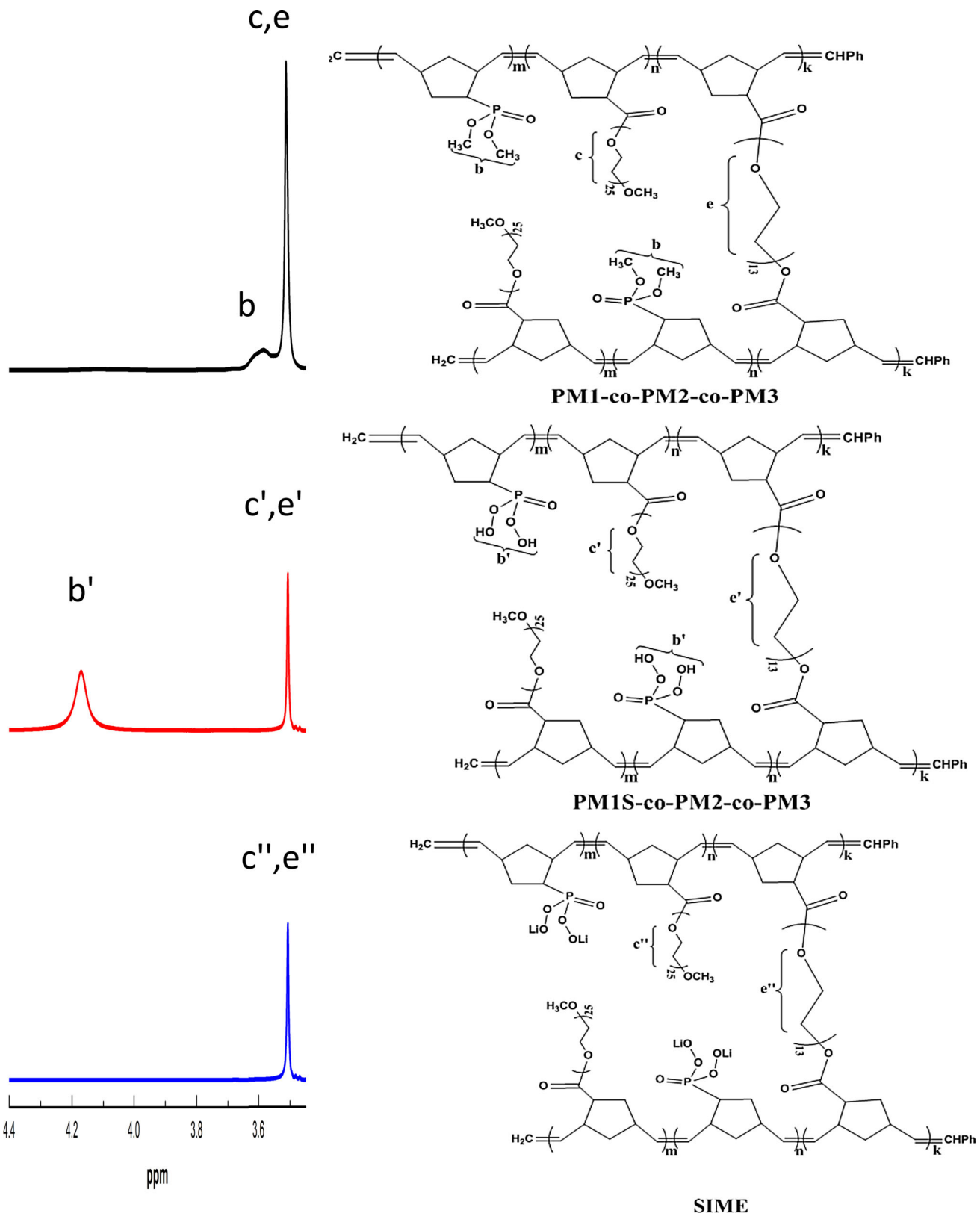

Fig. 3 Compared ^{1}H NMR characteristic peaks of phosphate ester group, phosphoric acid group, lithium phosphate group and structures of PM1-co-PM2-co-PM3, PM1S-co-PM2-co-PM3, SIME

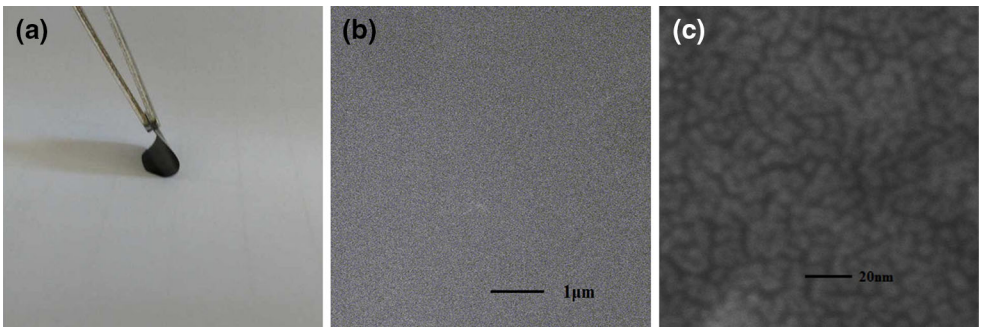

Fig. 4 **a** Photograph of the flexible nature of SIME, **b** SEM image of SIME magnified 1000 times and **c** SEM image of SIME magnified 300,000 times

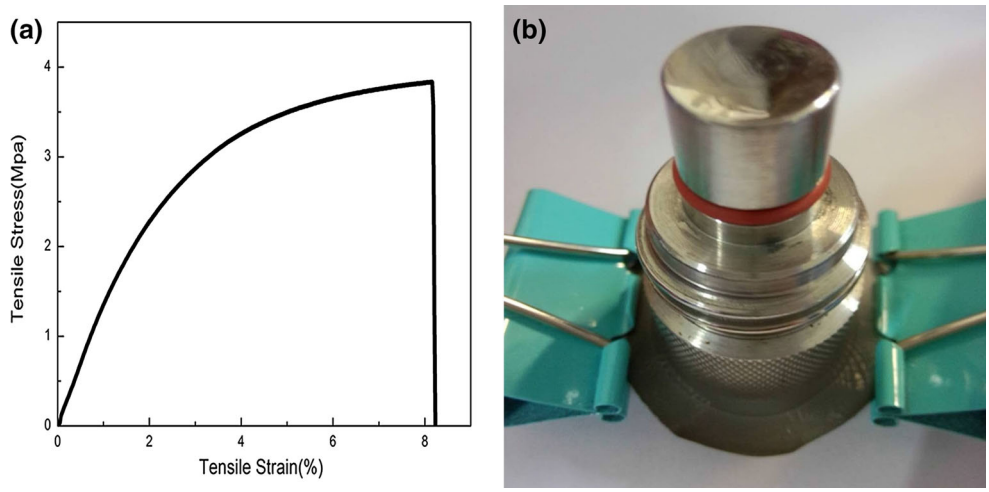

Fig. 5 **a** Tensile strength versus tensile strain graph of SIME and **b** photograph of the clamped SIME holding a stainless steel cylinder of 16 g of weight

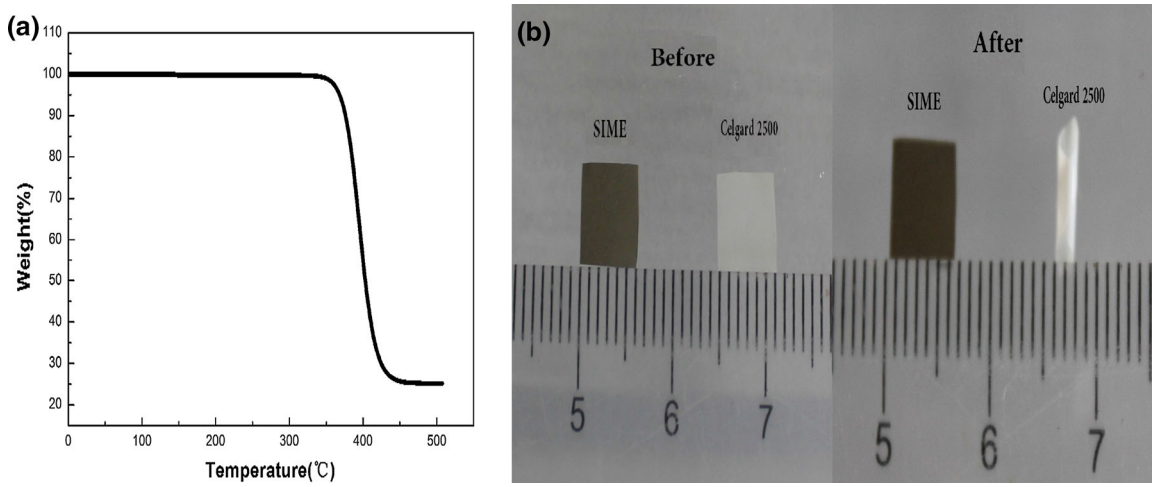

Fig. 6 **a** TGA of SIME (nitrogen, 5 °C min^{-1}, RT to 500 °C); **b** thermal shrinkage tests with SIME and Celgard 2500

ionic conductivity, mechanical robustness and thermal stability. In the stress–strain curve (Fig. 5a), the largest tensile strength of SIME is found to be 3.58 MPa with an elongation at break of 8.18%. Furthermore, it can successfully withstand stainless steel nuts of 16 g without any mechanical failure (Fig. 5b). Therefore, SIME satisfies the mechanical properties of an electrolyte membrane for battery assembly.

The thermal stability of electrolytes is a critical requirement for their safety and stability in lithium battery

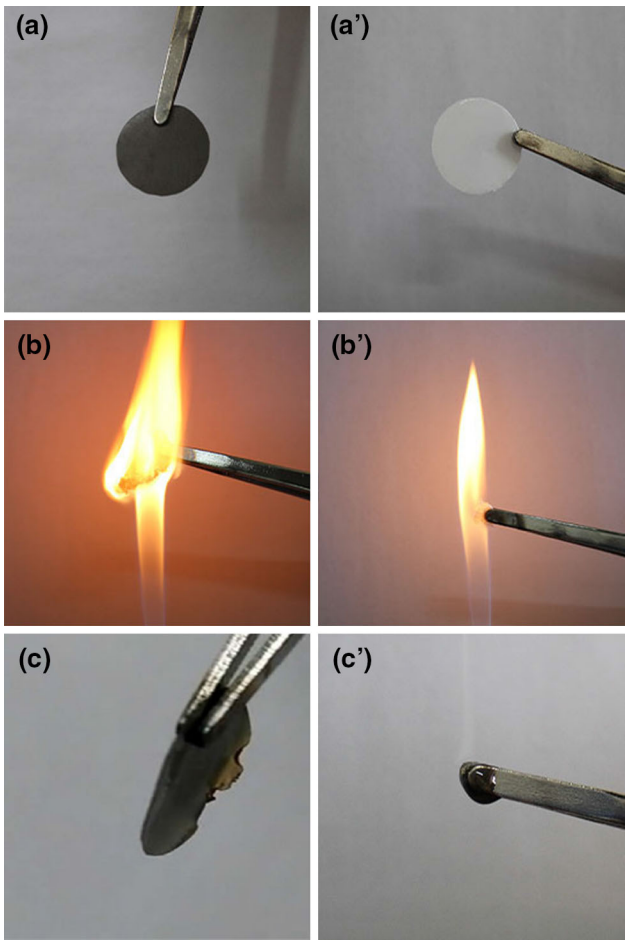

Fig. 7 Combustion test of the polymer membrane (**a**–**c**) and Celgard 2500 (**a′**–**c′**)

applications. The TGA curve of SIME is shown in Fig. 6a. No weight loss is observed until the temperature reaches roughly 350 °C, which indicates the prepared SIME has been completely separated from organic solvent. Subsequently the thermal degradation begins at 350 °C and extends up to 450 °C (ca. 75% of weight loss), due to the cleavage of chemical bonds. Given the exceedingly high initial degradation temperature up to 350 °C, it can be said that SIME exhibits superior thermal stability. Moreover, thermal deformation test of SIME compared with Celgard 2500 separator is employed at 180 °C for 2 h (Fig. 6b). Celgard 2500 separator exhibits significant shrinkage and curves up after thermal treatment, whereas SIME retains its original dimensions without shrinking and expanding. The above results show that SIME is potentially suitable for battery operation at elevated temperatures.

In the combustion test of Celgard 2500 and SIME, Celgard 2500 shrank immediately and caught on fire in a short time (<1 s) (Fig. 7b′) while SIME showed outstanding flame retardancy (Fig. 7b, c). The flame retardancy of SIME can be attributed to phosphonate group in the copolymer, and the retardant mechanism can be explained as follows [32, 33]: Firstly, when SIME was removed to heat or flame, the phosphorus group decomposed into phosphorus oxygen acid generator, followed by the formation of stable substance on the surface of polymer to prevent further combustion. Secondly, the phosphorus oxygen acid can promote the carbonation reaction and generate a lot of coke, whose poor thermal conductivity can delay heat transfer to the polymer matrix.

3.3 Electrochemical properties of SIME

The EIS plot of the electrolyte at room temperature is depicted in Fig. 8a, exhibiting a high-frequency semicircle followed by a low-frequency straight line, which corresponds to the bulk/grain boundary and the electrode resistance, respectively. And, the equivalent circuit used for fitting is depicted in the inset of Fig. 8a, wherein R1, R2, CPE and *W,* respectively, represent bulk resistance, interface resistance, constant phase element and Warburg resistance.

Based on the EIS plot, the ionic conductivity of SIME is calculated to be 1.31×10^{-4} S cm^{-1} at 20 °C and 5.67×10^{-4} S cm^{-1} and 80 °C, respectively, which falls into the range of conductivity displayed by most single-ion polymer electrolytes reported to date. As shown in Fig. 8b, the ionic conductivity dependence on the inverse of temperature (80–20 °C) displays a typical Arrhenius behavior. The high ionic conductivity is chiefly due to enhanced mobility of Li^+ ions resulting from extensive EO units contained in macromolecular framework of SIME. Moreover, the cross-linking inside SIME can reduce the crystallization of PEO and further afford easy motion of Li^+ ions.

Lithium ion transference number (T_{Li^+}) can be calculated according to the following equation [34]:

$$T_{Li^+} = \frac{I_s(\Delta V - I_0 R_0)}{I_0(\Delta V - I_s R_s)}$$

where I_0 and I_s are, respectively, the initial and final currents, while R_0 and R_s are the cell resistances before and after polarization. The values of variables required for the calculation are depicted in Table 1. T_{Li^+} of SIME was calculated to be 0.80 at room temperature, which stands for a typical single-ion conducting behavior [35]. Two main reasons can be introduced to explain why T_{Li^+} is not equal to unity [36, 37]. One is the short-range motions of negative charges in the flexible spacer between the main polymer chain and the attached anion, and the other is the segmental motions of the polyanionic block.

Linear sweep voltammetry (LSV) method is conducted at potentials from 2.0 to 6.0 V (vs. Li/Li^+) using Li/SIME/stainless steel cells at 20, 50 and 80 °C. As shown in Fig. 8c, the oxidative current onset increases with

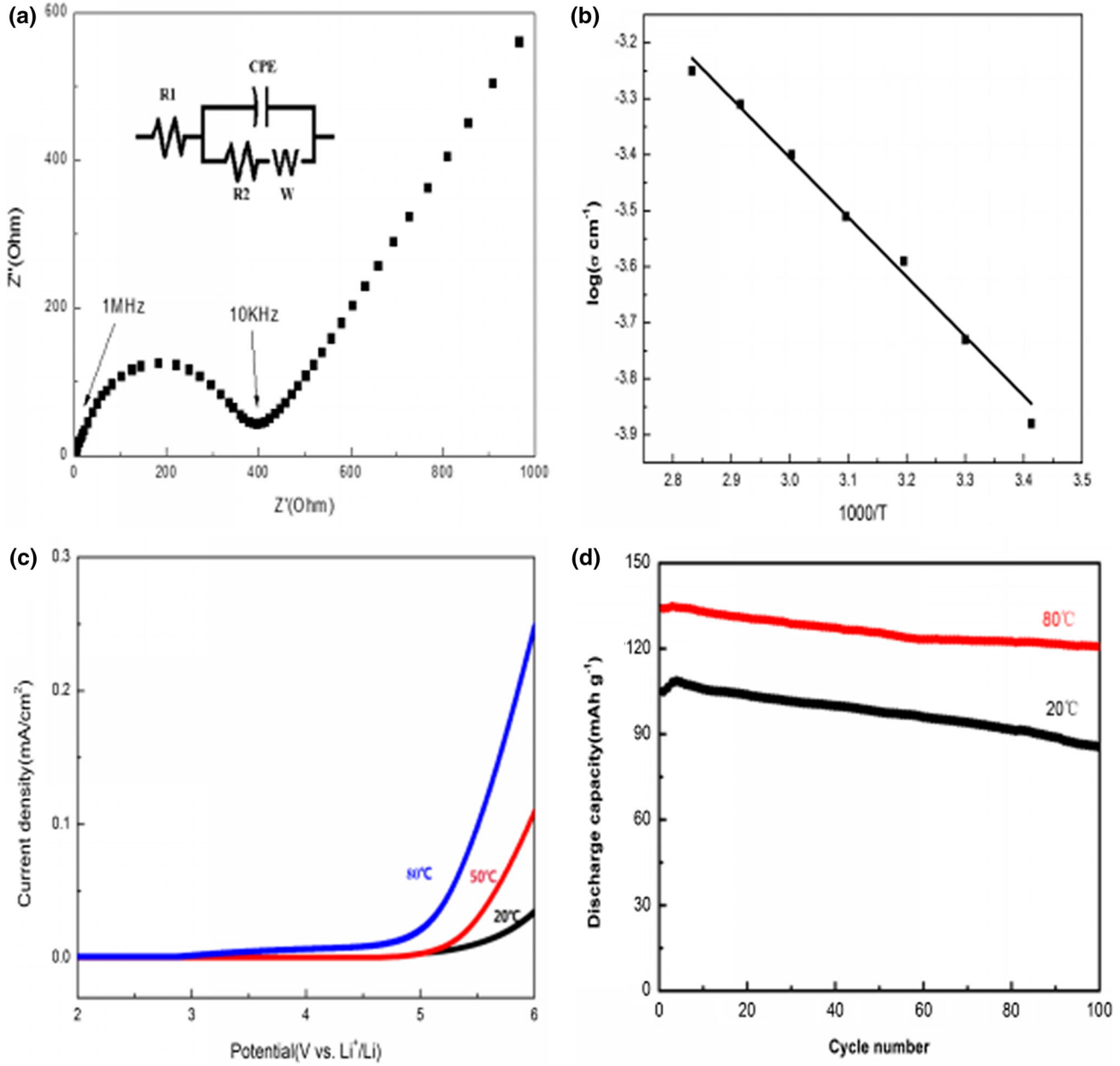

Fig. 8 **a** EIS plot of SIME at room temperature with the corresponding equivalent circuit, **b** Arrhenius plot of log(ionic conductivity) versus inverse absolute temperature, **c** linear sweep voltammograms of SIME at 20, 50 and 80 °C (scan rate 1 mV s^{-1}) and **d** long-term cycling stability $LiFePO_4$/SIME/Li cells at 20 and 80 °C with a 0.2 C-rate

Table 1 Parameters for calculation of lithium ion transference numbers (T_{Li^+})

ΔV (V)	I_0 (μA)	I_s (μA)	R_0 (Ω)	R_s (Ω)	T_{Li^+}
0.01	6.51	5.21	7.53	8.67	0.80

increasing temperature, while the electrochemical stability window is 5.5, 5.2 and 5.0 V, respectively, at 20, 50 and 80 °C. Simultaneously, along with the increasing temperature, the slope of current–voltage curves becomes greater, indicating that the test temperature affects the oxidation reaction kinetic. Overall, no significant oxidation current is observed below 5.0 V at three temperatures, indicating that the as-synthesized SIME is electrochemically stable up to 5.0 V. This result can be explained as follows: For SIME with a polyanionic structure, migrating and accumulating of the anions at the anodes are avoided, which reduces the concentration polarization and enhances the electrochemical stability [38]. So, it is promising to be applied in 5 V-class LIBs using cathode materials such as $LiNi_{0.5}Mn_{1.5}O_4$ or $LiCoPO_4$ at relatively high temperature.

Coin cells assembled with SIME, using $LiFePO_4$ as the cathode and Li metal as the counter anode, were fabricated to characterize its electrochemical performance. Discharge capacity versus cycle number of the coin cells at 20 and 80 °C with a 0.2 C-rate is compared in Fig. 8d. At 80 °C, discharge capacity of the cell is 134.1 mAh g^{-1} and is maintained at a value of 120.7 mAh g^{-1} after 100 cycles, 89.8% of its largest discharge capacity, whereas the cell examined at 20 °C delivers a smaller discharge capacity of 105.0 mAh g^{-1}, and the discharge capacity fades to 85.1 mAh g^{-1} at the 100th cycle. The increase in discharge capacity at a higher temperature can be attributed to the reduced resistance at the electrode–electrolyte interface. Moreover, the discharge capacity examined at 20 °C increased in the first few cycles, probably due to the steady formation of ordered channels for Li^+ ions conduction, while this phenomenon does not happen in the case at 80 °C, which can be due to an activation process of the active material and improvement in the adhesion contact between the electrolyte and the active material.

The superior cycling performance of SIME at higher temperature may be explained by various synergistic advantages originating from its molecular design. Firstly, the synthesis method using ROMCP enables the formation of a monodisperse and macromolecular electrolyte, leading to less boundary polarization and higher long-term electrochemical stability. Secondly, the flexibility of SIME can accommodate with the electrodes well, resulting in reduced resistance between electrodes and electrolyte. Finally, the chemical cross-linking reaction can form a stable three-dimensional network structure, limiting the deformation of SIME.

4 Conclusions

A flexible, high-voltage endurable and safe SIME has been successfully synthesized based on lithium phosphate, PEGME and PEG covalently bonded to polynorbornene chains. SIME exhibits good mechanical property, superior flame retarding, excellent thermal stability up to 350 °C. The ionic conductivity is 1.31×10^{-4} S cm^{-1} and 5.67×10^{-4} S cm^{-1}, respectively, at 20 and 80 °C. Moreover, SIME is electrochemically stable up to 5 V at 80 °C. The $LiFePO_4$/Li coin cell assembled with SIME delivers a high initial discharge capacity and performs well at 80 °C, with the discharge capacity fading 10.2% at 0.2 C-rate after 100 cycles. Further enhancement for electrochemical performance of the SIME can be envisaged by improving the regularity of its structure.

Acknowledgements This work was supported by National Natural Science Foundation of China (21574119) and Development Fund for Excellent Young Teacher of Zhengzhou University (1421324069).

References

1. Lin Y, Li J, Lai Y, Yuan C, Cheng Y, Liu J (2013) A wider temperature range polymer electrolyte for all-solid-state lithium ion batteries. RSC Adv 3:10722–10730
2. Shi Q, Xue L, Qin D, Du B, Wang J, Chen L (2014) Single ion solid-state composite electrolytes with high electrochemical stability based on a poly(perfluoroalkylsulfonyl)-imide ionene polymer. J Mater Chem A 2:15952–15957
3. Guhathakurta S, Min K (2010) Lithium sulfonate promoted compatibilization in single ion conducting solid polymer electrolytes based on lithium salt of sulfonated polysulfone and polyether epoxy. Polymer 51:211–216
4. Xu K (2004) Nonaqueous liquid electrolytes for lithium-based rechargeable batteries. Chem Rev 104:4303–4418
5. Johansson P (2001) First principles modeling of amorphous polymer electrolytes: Li^+–PEO, Li^+–PEI, and Li^+–PES complexes. Polymer 42:4367–4373
6. Pitawala H, Dissanayake M, Seneviratne V (2007) Combined effect of Al_2O_3 nano-fillers and EC plasticizer on ionic conductivity enhancement in the solid polymer electrolyte $(PEO)_9LiTf$. Solid State Ion 17:885–888
7. Cheng S, Smith D, Li C (2014) How does nanoscale crystalline structure affect ion transport in solid polymer electrolytes. Macromolecules 47:3978–3986
8. Zhang J, Huang X, Wei H, Fu J, Huang Y, Tang X (2010) Novel PEO-based solid composite polymer electrolytes with inorganic-organic hybrid polyphosphazene microspheres as fillers. J Appl Electrochem 40:1475–1481
9. Qian X, Gu N, Cheng Z, Yang X, Wang E, Dong S (2002) Plasticizer effect on the ionic conductivity of PEO-based polymer electrolyte. Mater Chem Phys 174:98–103
10. Kumar Y, Hashmi S, Pandey G (2011) Lithium ion transport and ion-polymer interaction in PEO based polymer electrolyte plasticized with ionic liquid. Solid State Ion 201:73–80
11. Wetjen M, Navarra M, Panero S, Passerini S, Scrosati B, Hassoun J (2013) Composite poly(ethylene oxide) electrolytes plasticized by N-Alkyl-N-butylpyrrolidinium Bis(trifluoromethanesulfonyl)imide for lithium batteries. ChemSusChem 6:1037–1043
12. Prasanth R, Shubha N, Hng H, Srinivasan M (2014) Effect of poly(ethylene oxide) on ionic conductivity and electrochemical properties of poly(vinylidenefluoride) based polymer gel electrolytes prepared by electrospinning for lithium ion batteries. J Power Sources 245:283–291
13. Aoki T, Konno A, Fujinami T (2004) Lithium ion conductivity of blend polymer electrolytes based on borate polymers containing fluoroalkane dicarboxylate and poly(ethylene oxide). Electrochim Acta 50:301–304
14. Park C, Sun Y, Kim D (2004) Blended polymer electrolytes based on poly(lithium 4-styrene sulfonate) for the rechargeable lithium polymer batteries. Electrochim Acta 50:375–378
15. Wang S, Min K (2010) Solid polymer electrolytes of blends of polyurethane and polyether modified polysiloxane and their ionic conductivity. Polymer 51:2621–2628
16. Brandell D, Kasemagi H, Tamm T, Aabloo A (2014) Molecular dynamics modeling the Li-PolystyreneTFSI/PEO blend. Solid State Ion 262:769–773
17. Lu Q, Fang J, Yang J, Yan G, Liu S, Wang J (2013) A novel solid composite polymer electrolyte based on poly(ethylene oxide) segmented polysulfone copolymers for rechargeable lithium batteries. J Membr Sci 425:105–112
18. Wang S, Hou S, Kuo P, Teng H (2013) Poly(ethylene oxide)-co-poly(propylene oxide)-based gel electrolyte with high ionic conductivity and mechanical integrity for lithium-ion batteries. Appl Mater Interfaces 58:477–8485

19. Itoh T, Fujita K, Inoue K, Iwama H, Kondoh K, Uno T, Kubo M (2013) Solid polymer electrolytes based on alternating copolymers of vinyl ethers with methoxy oligo(ethyleneoxy)ethyl groups and vinylene carbonate. Electrochim Acta 112:221–229
20. Kang E, Jung H, Park J, Kwon S, Shim J et al (2011) Block copolymer directed one-pot simple synthesis of L10-Phase FePt nanoparticles inside ordered mesoporous aluminosilicate/carbon composites. J ACS Nano 5:1018–1025
21. Wang J, Woo S, Shim J, Jo C, Lee K (2013) One-pot synthesis of tin-embedded carbon/silica nanocomposites for anode materials in lithium-ion batteries. J ACS Nano 7:1036–1044
22. Nakanishi K, Tanaka N (2007) Sol–gel with phase separation hierarchically porous materials optimized for high-performance liquid chromatography separations. Acc Chem Res 40:863–873
23. Young W, Epps T (2012) Ionic conductivities of block copolymer electrolytes with various conducting pathways: sample preparation and processing considerations. Macromolecules 45:4689–4697
24. Jo G, Ahn H, Park M (2013) Simple route for tuning the morphology and conductivity of polymer electrolytes: one end functional group is enough. ACS Macro Lett 2:990–995
25. Jo G, Jeon H, Park M (2015) Synthesis of polymer electrolytes based on poly(ethylene oxide) and an anion-stabilizing hard polymer for enhancing conductivity and cation transport. ACS Macro Lett 4:225–230
26. Scrosati B (2010) Lithium batteries: status, prospects and future. J Power Sources 195:2419–2430
27. McOwen D, Seo D, Borodin O, Vatamanu J et al (2014) Concentrated electrolytes: decrypting electrolyte properties and reassessing Al corrosion mechanisms. Energy Environ Sci 7:416–426
28. Wang X, Liu Z, Zhang C, Kong Q, Yao J et al (2013) Exploring polymeric lithium tartaric acid borate for thermally resistant polymer electrolyte of lithium batteries. Electrochim Acta 92:132–138
29. Xu G, Zhang Y, Rohan R, Cai W, Cheng H (2014) Synthesis, characterization and battery performance of a lithium poly (4-vinylphenol) phenolate borate composite membrane. Electrochim Acta 139:264–269
30. Zhang Y, Lim C, Cai W, Rohan R, Xu G et al (2014) Design and synthesis of a single ion conducting block copolymer electrolyte with multifunctionality for lithium ion batteries. RSC Adv 4:43857–43864
31. Zhang Y, Rohan R, Cai W, Xu G, Sun Y, Lin A, Cheng H (2014) Influence of chemical microstructure of single-ion polymeric electrolyte membranes on performance of lithium-ion batteries. Appl Mater Interfaces 6:17534–17542
32. Qian L, Ye L, Qiu Y, Qu S (2011) Thermal degradation behavior of the compound containing phosphaphenanthrene and phosphazene groups and its flame retardant mechanism on epoxy resin. Polymer 52:5486–5493
33. Levchik S, Weil E (2006) A review of recent progress in phosphorus-based flame retardants. J Fire Sci 24:345–364
34. Evans J, Vincent C, Bruce P (1987) Electrochemical measurement of transference numbers of polymer electrolytes. Polymer 28:2324–2328
35. Ye Y, Wang H, Bi S, Xue Y, Xue Z, Zhou X, Xie X, Maib Y (2015) High performance composite polymer electrolytes using polymeric ionic liquid-functionalized graphene molecular brushes. J Mater Chem A 3:18064–18073
36. Porcarelli L, Shaplov AS, Salsamendi M, Nair JR, Vygodskii YS, Mecerreyes D, Gerbaldi C (2016) Single-ion block copoly(ionic liquid)s as electrolytes for all-solid state lithium batteries. ACS Appl Mater Interfaces 8:10350–10359
37. Liu Y, Yf Zhang, Pan M, Xp Liu, Cc Li, Yb Sun, Dl Zeng, Hs Cheng (2016) A mechanically robust porous single ion conducting electrolyte membrane fabricated via self-assembly. J Membr Sci 507:99–106
38. Teran A, Mullin S, Hallinan D, Balsara N (2012) Discontinuous changes in ionic conductivity of a block copolymer electrolyte through an order–disorder transition. ACS Macro Lett 1:305–309